Journal of Rare Earths 37 (2019) 101–112

Contents lists available at ScienceDirect

Journal of Rare Earths

journal homepage: http://www.journals.elsevier.com/journal-of-rare-earths

Flotation behavior and electronic simulations of rare earth minerals in the presence of dolomite supernatant using sodium oleate collector☆

E.R.L. Espiritu [a], G.R. da Silva [a], D. Azizi [b], F. Larachi [b], K.E. Waters [a,*]

[a] Department of Mining and Materials Engineering, McGill University, 3610 University Street, Montreal, Quebec H3A 0C5, Canada
[b] Department of Chemical Engineering, Université Laval, 1065 Avenue de La Médecine, Québec, Québec G1V 0A6, Canada

ARTICLE INFO

Article history:
Received 21 January 2018
Received in revised form
26 April 2018
Accepted 26 April 2018
Available online 11 August 2018

Keywords:
Rare earth minerals
Bastnäsite
Monazite
Dolomite
Sodium oleate
DFT simulation

ABSTRACT

Common rare earth (RE) minerals, such as bastnäsite and monazite, may be formed in deposits associated with carbonate gangue, such as calcite and dolomite. Sodium oleate is a widely used collector for the flotation of both RE and gangue minerals, which might, therefore, be an inefficient process due to the lack of selectivity of this collector. Since these minerals are also sparingly soluble in solution, they could release their constituent ions into the solution, which could affect the floatability of other minerals. In this study, the interactions of sodium oleate with bastnäsite and monazite in the presence of dissolved dolomite species have been investigated. Microflotation tests were carried out to explore the effects of these dissolved species on the floatability of the RE minerals. Zeta potential measurements and XPS characterization were carried out to understand how the species affect the collector adsorption. To complement these characterizations, density functional theory (DFT) simulations were conducted to investigate the collector-mineral and collector-adsorbed species (on the mineral surface) interactions. The results show that collector-dolomite interaction energy is greater than that of collector-adsorbed species, but lower than collector-monazite interaction energy, explaining the decrease in the minerals' recovery upon exposure to the dissolved mineral species. It is also shown that oleate ions (Ol^-) have the strongest interaction with the minerals compared to other oleate species such as acid soap (HOl_2^-) and oleate dimer (Ol_2^{2-}). The behavior (strength and selectivity) of sodium oleate towards RE minerals and dolomite, as compared to other RE mineral collectors (such as aromatic hydroxamate), is attributed mainly to the collector's and the minerals' structure. The long hydrocarbon chain of sodium oleate which imparts hydrophobic characteristic to the minerals, makes it stronger collector than benzohydroxamate. Moreover, sodium oleate (with linear structure), unlike the aromatic hydroxamate, can approach the mineral easier due to lesser steric hindrance effect and higher reactivity of O involved in the interaction, making it less selective. In addition, it can interact easily with dolomite due to the presence of more exposed active sites than RE minerals.

1. Introduction

Sodium oleate, an oxyhydryl collector, is a widely used industrial collector[1] especially for non-sulphide minerals.[2] This type of collector floats a variety of non-sulphide minerals such as Ca-, Ba-, and Mg-containing minerals, non-ferrous carbonates, the soluble salts of alkali and alkaline earth metals[2] and even rare earth (RE) minerals.[3–5] Main RE minerals, such as bastnäsite and monazite, usually occur associated with carbonate gangue such as calcite and dolomite. Since this is the case, RE flotation using only sodium oleate is inefficient due to the non-selectivity of the collector.[6] In addition, the carbonate gangue and RE minerals are sparingly soluble in water,[7] which means that constituent ions from the minerals could be dissolved in the solution. Although RE minerals are usually associated with semi-soluble carbonate minerals, surprisingly the effect of the dissolved mineral species on RE minerals has barely been investigated in the open literature. These ions are reported to possibly interact with the RE mineral surface affecting their flotation behavior.[8,9] In this regard, the possible interaction of sodium oleate with mineral surfaces has been studied to

☆ **Foundation item**: Project supported by the Natural Sciences and Engineering Research Council of Canada (NSERC) and Niobec, a Magris Resources Company through the Collaborative Research and Development Program (CRDPJ 453164-13).
* Corresponding author.
E-mail address: kristian.waters@mcgill.ca (K.E. Waters).

https://doi.org/10.1016/j.jre.2018.04.016
1002-0721/

understand interfacial interactions.[10,11] Although this is a widely-studied collector, there are relatively few investigations involving RE minerals- more work has been conducted on calcite and other gangue minerals. The interaction of sodium oleate with calcite and other gangue minerals have been studied extensively. Somasundaran and Ananthapadmanbhan[12] have presented the formation of various oleic acid species in solution and its possible correlation to flotation performance. They highlighted the possible role of acid soap (HOl_2^-) in the increase in flotation of hematite in the alkaline pH range. They also mentioned that neutral oleic acid (HOl) could adsorb through hydrogen bonding with surface hydroxyl groups or co-adsorption between the ionic species. Others reported similar findings where mineral's maximum recovery occurs at pH between 7 and 9 in the presence of oleate.[13,14] They attributed the high recovery to the maximum activity of oleate caused by the presence of acid soap complex in this pH region. Maximum recovery of RE minerals in the presence of sodium oleate were also found to occur at this pH range,[15,16] but the interaction of these complexes with RE minerals have not been discussed comprehensively.

Typical methodologies to understand the mechanism of the adsorption of the collector onto the RE minerals involving dissolved mineral species (in the solution) includes surface characterization (e.g., FTIR and XPS) and electrokinetic tests (e.g., zeta potential measurements). However, some of the results could have discrepancies since these measurements are seldom conducted *in situ*. In this regard, atomically-resolved computer simulations such as density functional theory (DFT) simulations could strengthen the inferences from these experimental results. DFT simulations could contribute further understandings of the mineral flotation behavior in the presence of supernatant that cannot be directly achieved by experiments. It has been reported that molecular modelling has been helpful in understanding mineral-reagent interactions,[17–20] because it can provide valuable information even without detailed experimental testing.[21] With regard to oleate adsorption on mineral surfaces, several molecular modelling studies have already been presented in the literature.[19,21] However, these computer simulations were conducted solely with oleate (Ol^-) and not the other possible oleate species that could also be present in the solution such as oleate dimer (Ol_2^{2-}) and acid soap (HOl_2^-).[14]

Therefore, an integrated experimental and DFT simulation study was conducted not only with oleate but also with the consideration of other oleate species (e.g., acid soap and oleate dimer) in order to make this study more comprehensive. In this work, the effects of dissolved ions from dolomite on the flotation of RE minerals, bastnäsite and monazite, were investigated through microflotation tests. These were rationalized with the help of zeta potential measurements, XPS analyses and DFT simulations.

2. Experimental

2.1. Materials

African Rare Earths (Pty.) Ltd. (South Africa) provided the bastnäsite. Monazite (Eureka Farm 99, Namibia) and dolomite (Sterling Hill Mine, New Jersey) were purchased from Mineralogical Research Company (USA) and Boreal Science (Canada), respectively. X-ray diffraction (XRD) analysis and inductively coupled plasma-optical emission spectroscopy (ICP-OES) for mineral and elemental analysis, respectively, indicated that the dolomite and bastnäsite are relatively pure, while monazite sample has minor calcite contamination.[9] The elemental analysis is presented in Table 1.

The sodium chloride (supporting electrolyte), the hydrochloric acid and potassium hydroxide (pH modifiers) and the sodium oleate (NaOl) collector were obtained from Fisher Scientific (Canada).

The dolomite supernatant was obtained by conditioning 75 g of dolomite in 1500 mL deionised water for 8 h at 60 °C. The suspension was allowed to cool before passing through a filter with a particle retention of 5 μm to recover the supernatant. The measured conductivities of the deionised water and supernatant were found to be 5 and 90 μS, respectively. The amounts of Ca^{2+} and Mg^{2+} in the supernatant were analyzed using Varian AA240FS Fast Sequential Atomic Absorption Spectrometer (Agilent Technologies, USA) and observed to be 8.07 and 3.54 ppm, respectively. Deionised water was used as the blank for this measurement. It must be noted that these Ca and Mg contents are lower than typical tap water concentrations.

2.2. Zeta potential measurements

The mineral samples used for zeta potential measurements (dolomite, monazite and bastnäsite) have a D_{50} of 2.3 μm. The minerals are placed in a pre-adjusted solution of 1×10^{-3} mol/L NaCl (indifferent electrolyte) or dolomite supernatant. The solution pH was adjusted using dilute concentrations of HCl and KOH. For the measurements with the collector, the minerals were first conditioned with supernatant for 0, 30, 60, 120 and 240 s, then with the collector for another 240 s. The 100 mg/L mineral suspension was mixed prior to the measurement to ensure particle dispersion. Zeta potential measurements were then taken using a NanoBrook 90Plus zeta particle size analyzer (Brookhaven Instruments, USA).

2.3. Flotation

A modified Hallimond tube, as presented and described previously,[9] was used for the microflotation tests. One gram (1 g) of -106 + 38 μm mineral sample was placed in a 50-mL beaker containing 30 mL deionised water or dolomite supernatant (pre-adjusted to desired pH). The suspension was conditioned for 2 min with dolomite supernatant then 5 min with 3.3×10^{-5} mol/L (or 10 mg/L) sodium oleate collector, while keeping the pH constant. The mineral particles were kept suspended by employing a magnetic stirrer. The suspension was then added to the cell and further completed up to 170 cm^3 with pH-adjusted deionised water. Air was introduced at a flowrate of 40 mL/min and the flotation test was conducted for 1 min.

2.4. Density functional theory (DFT) simulations

All DFT-based calculations were performed using Dmol3 package implemented in the Material Studio 2016 software. Through DFT simulations, geometric crystal parameters and total energy of dolomite and monazite optimized bulk structures, their free surfaces considering their most stable cleavage planes, model oleic acid collector, and adsorbed collector and species from dolomite supernatant onto mineral surfaces were calculated.

The generalized gradient approximation (GGA) with PBEsol exchange correlation functional was used to describe the exchange correlation interactions. Calculations were performed using the double numerical plus polarization (DNP) basis set and the spin-unrestricted assumption. The self-consistent filed (SCF) convergence was fixed to 2×10^{-6} and convergence criteria set for the energy, maximum force and maximum displacement were set to 2×10^{-5} Ha, 0.5 Ha/nm, and 0.02 nm, respectively. It is worth mentioning that the simulation results with fixed SCF value in 1×10^{-6} were the same with simulations with SCF value equals to 2×10^{-6}. No special treatment of core electrons was considered, and all the electrons were included in the calculations. Also,

smearing was set to 5×10^{-3} through all calculations. In this condition, the calculation was performed by use of various orbitals for different spins. Besides, the initial value for the number of unpaired electrons for each atom was taken from the formal spin introduced for each atom. In this situation, the starting value can be subsequently optimized throughout calculations. For minerals bulk calculations, the Brillouin zone was sampled using a $(2 \times 2 \times 2)$ Monkhorst-Pack *k*-point mesh. This mesh value has been selected after systematic simulation studies using finer values. It was found the simulation results with *k*-point mesh $(2 \times 2 \times 2)$ are highly close to results with finer values, with lesser simulation time. The most stable cleavage planes for dolomite and monazite were taken for calculations. In this regard, the cleavage plane (104) for dolomite and (100) for monazite, which both agree with the literature values,[8,22,23] were used.

The mineral slabs were constructed by (1×2) dolomite (104) and monazite (100) surface supercells with 4 nm vacuum spacing to prevent interaction between image slabs. Since flotation occurs in an aqueous environment, all the simulations were performed using the conductor-like screening model (COSMO) as an implicit solvation model. It should be noted that the convergence of bastnäsite (104) slab was not achieved using COSMO. As simulations should be performed by COSMO to mimic the aqueous environment in froth flotation, bastnäsite simulation is not presented in this work. In COSMO, the solute molecules form a cavity within a dielectric continuum of permittivity equal to water's permittivity. During adsorption calculations of either collector or supernatant species on the mineral surfaces, the atoms at the top layer were allowed to undergo relaxation and the rest of atoms in sub-layers were constrained. This is because only the mineral surface top-layer atoms are likely to interact with oleic acid collector and other species through adsorption. The adsorption energy of either collector or adsorbed species onto the mineral surfaces was calculated based on the following definition[20]:

$$E_{ads} = E_{(slab+collector\ or\ adsorbed\ species)} - E_{(slab)} - E_{(collector\ or\ adsorbed\ species)} \quad (1)$$

where $E_{(slab+collector\ or\ adsorbed\ species)}$ is the total interaction energy after adsorption of either collector or adsorbed metal cation species on the mineral surface, $E_{(slab)}$ represents the energy of relaxed bare mineral slab and $E_{(collector\ or\ adsorbed\ species)}$ is the energy of collector or adsorbed metal cation/species after optimization.

In the cases where the collector interacts with adsorbed metal cation species onto the mineral surfaces, the interaction energy was calculated as follows:

$$E_{ads} = E_{(slab+collector+adsorbed\ species)} - E_{(slab)} - E_{(collector)} - E_{(adsorbed\ species)} \quad (2)$$

3. Results

3.1. Zeta potential measurements

Dolomite, monazite and bastnäsite were conditioned with dolomite supernatant for 0, 30, 60, 120 and 240 s. The zeta potential was then measured in the presence of sodium oleate and is presented in Fig. S1 (see Supplementary Information). The result indicated that the zeta potential is greatly influenced by the presence of the supernatant at pH 7 and 9. Since previous studies have shown that maximum recovery of RE minerals in the presence of oleate occurred at pH close to 7,[15,16] further zeta potential measurements were conducted at this pH value. The measurements at pH 7, presented in Fig. 1, showed that dolomite has a negative zeta potential (−10 mV); monazite has slightly negative potential (−0.6 mV); while bastnäsite has a positive zeta potential (9.8 mV). The measurements with NaOl collector (−29, −25 and −35 mV, respectively) suggest that collector was adsorbed at the surface of each mineral. It can also be seen that the presence of dolomite supernatant has caused the zeta potential of the minerals to become less negative (Fig. 1). This behavior is similar to that observed in the previous study[9] at pH 9. When the minerals conditioned with supernatant were put in contact with the collector, their zeta potential values became more negative than only with the presence of supernatant (but not as negative as only with the presence of NaOl), indicating that the collector could still adsorb onto the minerals' surface.

3.2. Microflotation

The effect of dolomite supernatant on the floatability of dolomite, monazite, and bastnäsite was also studied through microflotation tests. In Fig. 2, the recovery of the minerals with and without dolomite supernatant is presented, where the error bars represent 95% confidence interval. The recovery of dolomite conditioned with the collector in deionised water and in dolomite supernatant is 69% and 66%, respectively. The presence of the supernatant does not seem to affect dolomite's floatability in the presence of NaOl collector, which is similar with the result presented in the presence of benzohydroxamate at pH 9.[9] However, the presence of dolomite supernatant has clearly influenced the floatability of the other minerals, reducing the recovery of monazite and bastnäsite from 98% and 99% to 57% and 51%, respectively (see Fig. 2).

3.3. Speciation

Since dolomite supernatant was used, it is important to understand its speciation in the solution. In this regard, the equilibria for dolomite-water-CO_2 system were considered[24] (see Eqs. S1–S17 in Supplementary Information C). The speciation diagrams (Fig. S2) indicated that $MgCO_3$, $CaCO_3$, $Mg(OH)_2$ and $Ca(OH)_2$ precipitates could be present at pH 7. The species can be formed at the solution/

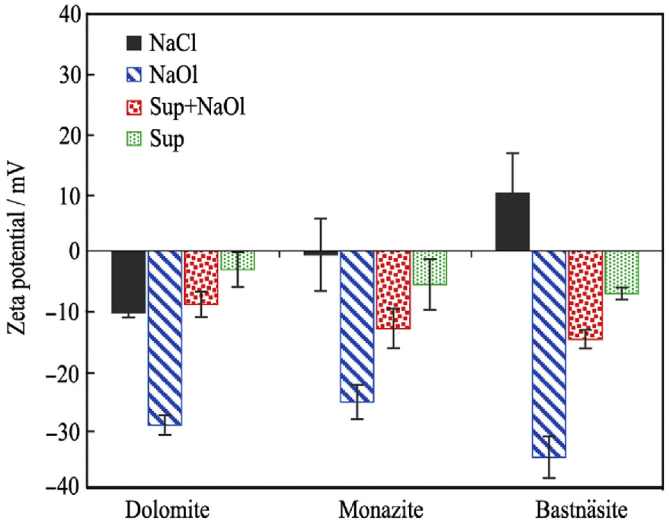

Fig. 1. Zeta potential of dolomite, monazite, and bastnäsite in the presence of 1×10^{-3} mol/L NaCl (background electrolyte), with 3.3×10^{-5} mol/L NaOl, with supernatant and NaOl, and with only supernatant at pH 7.

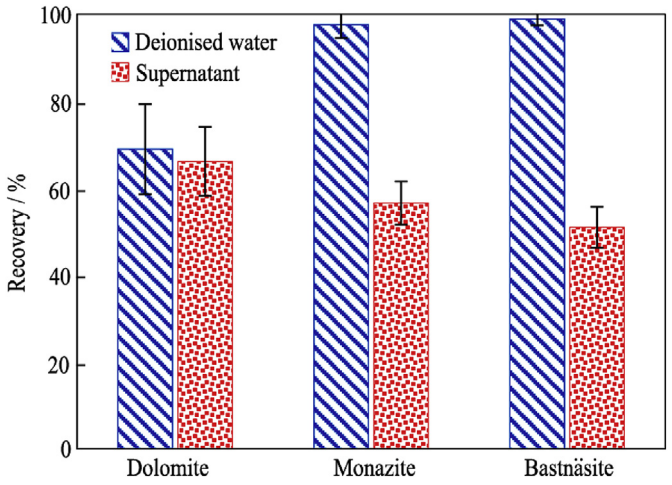

Fig. 2. Microflotation results of dolomite, monazite, and bastnäsite using 3.3×10^{-5} mol/L NaOl in deionised water and dolomite supernatant at pH 7.

surface interface or in the solution and then adsorbed at the surface.[25]

The speciation diagram of oleate (Fig. 3(a) and (b)) was also plotted using HySS2009 software (Protonic software).[26] The speciation of oleate was based on the data provided by Somasundaran and Ananthapadmanbhan,[12] where the reported pK_s (conversion of liquid to aqueous) is 7.6 and acid dissociation constant (pK_a) is 4.95. The presence of Ca and Mg ions led to the formation of Ca- and Mg-oleate precipitates.

3.4. DFT simulations

DFT simulations have been carried out to objectify the interaction of oleic acid collector species in aqueous phase on the RE minerals and dolomite surfaces, as well as RE minerals in the presence of dolomite supernatant. As the behaviors of both monazite and bastnäsite were comparable through flotation studies, it was decided, for the sake of brevity, to use only monazite for DFT simulation. Dolomite as a carbonatite gangue mineral was also considered for comparisons with monazite results.

The solution chemistry of oleic acid in aqueous phase reveals that this collector dissociates in three main species including, oleate ions $(Ol)^-$, oleate dimer $(Ol)_2^{2-}$, and acid soap $H(Ol)_2^-$.[14] Thus, their electronic properties and interaction with mineral surfaces will be discussed first. Among these species, the focus will be on oleate ion as it is the most abundant form at the pH investigated (Fig. 3).

3.4.1. Optimised structure of oleate ion, oleate dimer and acid soap

The structure of oleate ion was first optimized by DFT simulations to understand its reactivity and the nature of its interaction with mineral surfaces. Oleic acid is dissociated into an ionic form in aqueous solutions at pH > 5.[27] The geometry of the ionic form of the collector after optimization is shown in Fig. 4(a) with C–O and C=O bond lengths of 0.128 nm, and O=C–C bond angles of 120.14°. Likewise, the highest occupied molecular orbitals (HOMOs) and the lowest unoccupied molecular orbitals (LUMOs) of oleate ion are shown in Fig. 4(b) and (c), respectively. These HOMOs and LUMOs in oleate ion polar head are responsible for the collector interaction with the minerals surfaces through exchange of electrons with HOMOs and LUMOs on the minerals' surfaces. In this regard, the oleate ion can transfer its HOMO electrons to LUMOs of metal atoms on the mineral surfaces to form covalent bond. Conversely, if the metal atoms can transfer some of their electrons to the oleate ion LUMOs back-donation covalent bond may also be formed increasing interaction between collector and mineral surfaces.[28] As seen in Fig. 4(a–c), oleate ion has the potential for both donating and accepting electrons through bond formation via either HOMOs or LUMOs in its structure.

The collector's transferable charges are mostly located on its polar head bearing the functional group (carboxyl functional group) (see Fig. 4). In addition, the polar head has an ability to accept electrons attributed to its LUMOs. In this regard, the average charge of O atom on both C=O and C–O functional groups amounts to −0.50e based on the Mullikencharge analysis. This indicates that the two O atoms are active centers in the collector polar head to enable the two functional groups to be involved in collector-mineral interactions. Through adsorption, electrons from the negatively charged ions can be shared with mineral surfaces through covalent bonding. The charges of O on each of C=O and C–O contribute for −0.41e and −0.58e, respectively, indicating that oxygen atom in C–O has a stronger coordination ability with the metal ions as compared to the carbonyl O.

The optimized structures of acid soap $H(Ol)_2^-$ and oleate dimer $(Ol)_2^{2-}$ were also calculated through DFT simulations (see Fig. 4). A higher distribution of LUMOs and HOMOs is found for $H(Ol)_2^-$.

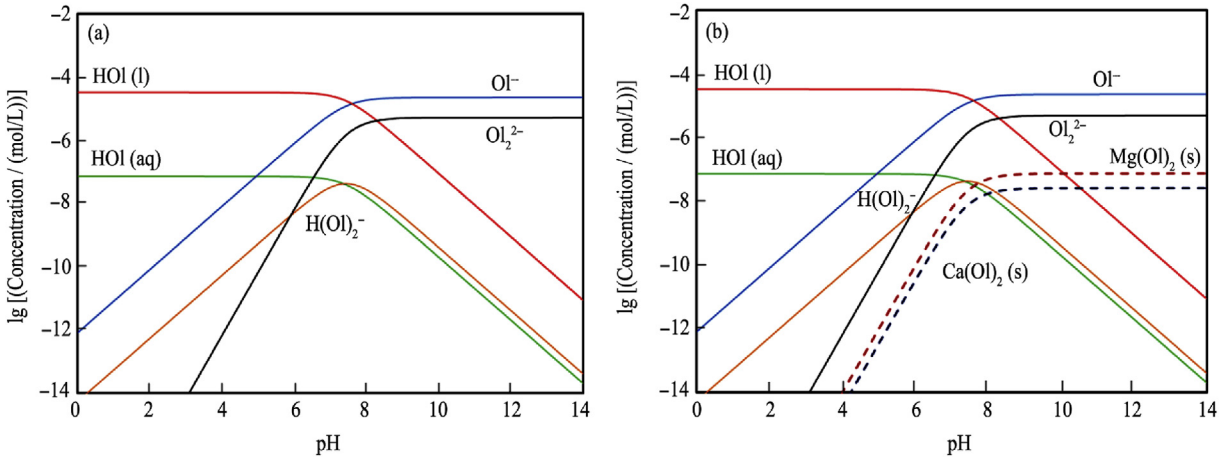

Fig. 3. Speciation diagram for oleate system without (a) and with (b) Ca and Mg ions. Total concentration: $[Ol^-]_{TOT} = 3.3 \times 10^{-5}$ mol/L, $[Ca^{2+}]_{TOT} = 2 \times 10^{-4}$ mol/L, and $[Mg^{2+}]_{TOT} = 1.5 \times 10^{-4}$ mol/L at $T = 25$ °C.

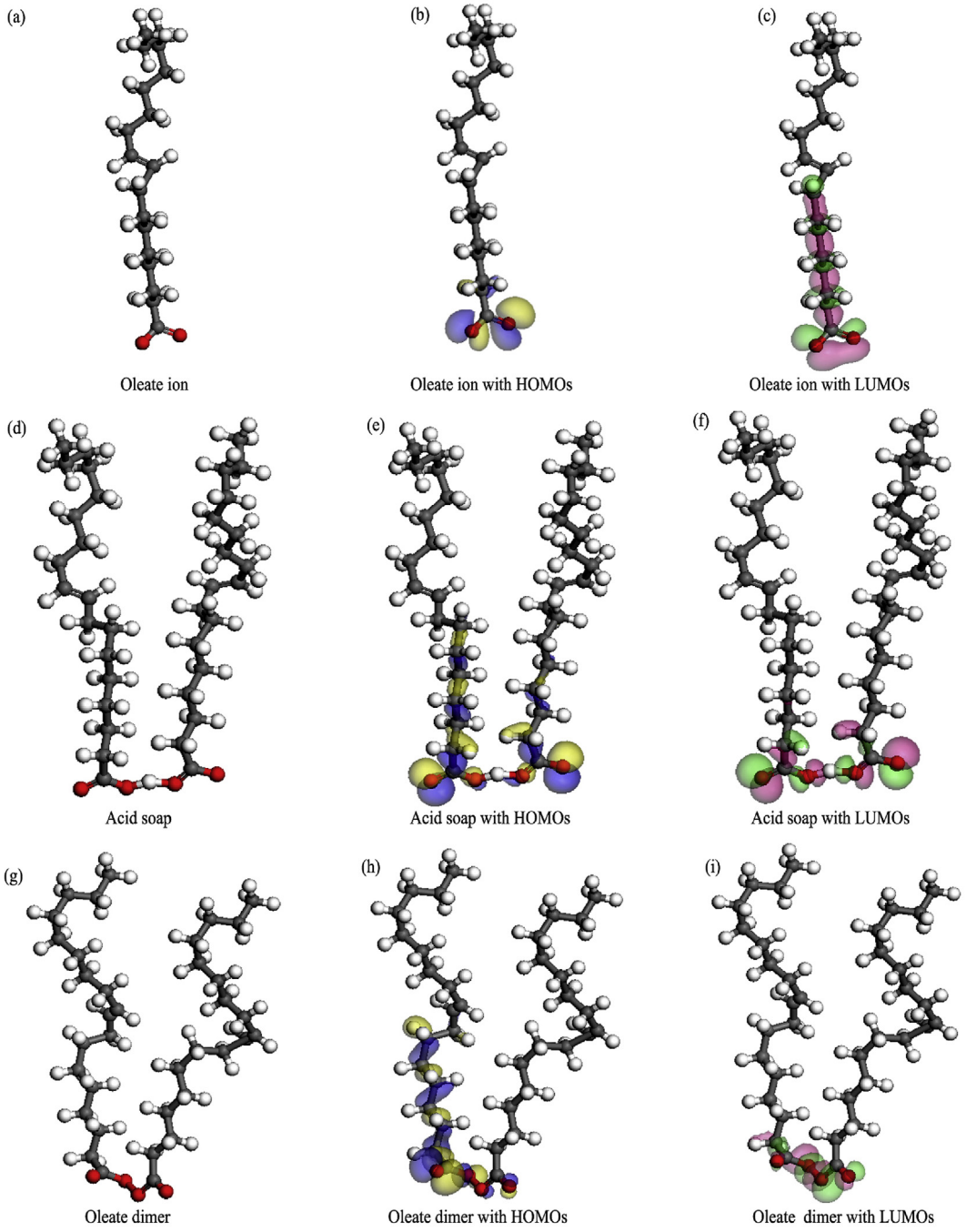

Fig. 4. DFT optimized structures for the different oleic acid species in aqueous solution and their corresponding structures with HOMOs and LUMOs (O ≡ red, C ≡ gray, H ≡ white).

This latter species exhibits higher activity as compared with the oleate dimer. This higher activity can be captured from a Mulliken charge analysis: oxygen atoms in acid soap polar head (C=O and C–O functional groups) are −0.37e, −0.50e, −0.49e, and −0.36e (average = −0.43e), from left to right, respectively (Fig. 4(d)); while for oleate dimer oxygen these charges were −0.40e, −0.22e, −0.23e, and −0.40e (average = −0.31e), from left to right, respectively (Fig. 4(g)). The average negative charge of oxygen atoms in C=O and C–O groups of oleate ions (−0.5e) exceeds that of either acid soap or oleate dimer suggesting the following order of interaction strength: oleate ions $(Ol)^-$ > acid soap $H(Ol)_2^-$ > oleate dimer $(Ol)_2^{2-}$.

3.4.2. Collector-mineral surface interactions

3.4.2.1. Case of oleate ion on monazite and dolomite surface. Fig. 5(a) and (b) illustrate the geometrical details of the interaction of oleate ion with bare monazite and dolomite surfaces, respectively. Either C=O or C–O group interacts with Ce atoms on monazite surface through covalent bonding (Fig. 5(a)). This type of bonding can be confirmed by the interaction energy, bond lengths and Mulliken charge analysis. The collector-monazite interaction energy amounts to −422.2 kJ/mol (as seen in Table 4) is large enough favoring chemical type of interaction. Moreover, the O–Ce distances between C–O and C=O groups and surface Ce atoms are *ca.* 0.224 and 0.223 nm, respectively. These collector-mineral bond

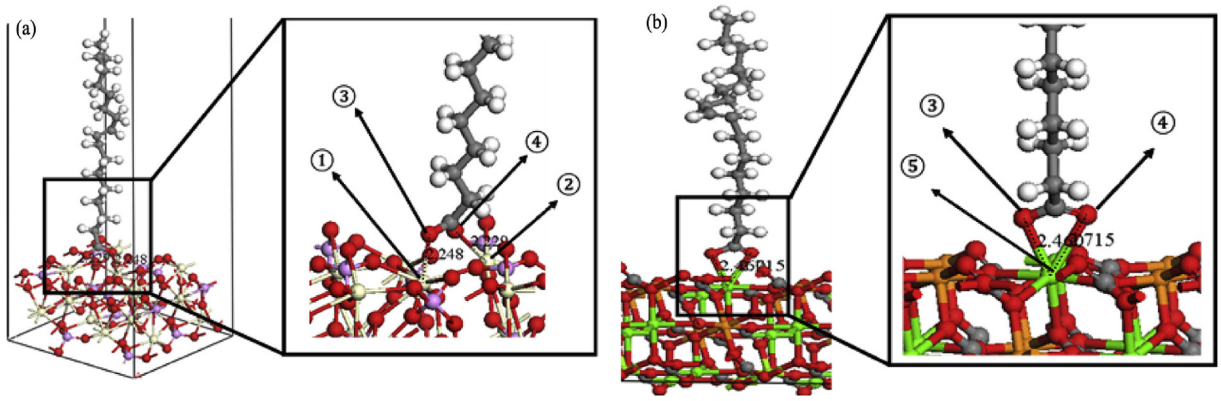

Fig. 5. Interaction of oleate ion onto monazite surface (100) (a) and dolomite surface (104) (b) (Ce ≡ beige, O ≡ red, P ≡ purple, C ≡ gray, Mg ≡ orange, Ca ≡ green, H ≡ white).

Table 1
Chemical compositions (wt%) of dolomite, monazite and bastnäsite samples.

Dolomite	Ca	Mg	Fe	S	Mn	Na	K	Tl	Cu	Zn	Mo
	21.71	12.74	0.366	0.209	0.059	0.052	0.035	0.029	0.020	0.017	0.012
Monazite	P	Ce	Nd	La	Ca	Si	Pb	Zr	Fe	Al	As
	10.24	8.00	5.41	4.64	0.748	0.511	0.486	0.457	0.116	0.100	0.100
Bastnasite	Ce	La	Nd	As	P	Tl	Fe	Ca	Al	Pb	Cu
	13.55	13.44	8.08	0.688	0.534	0.379	0.251	0.211	0.183	0.089	0.064

Table 2
Mulliken charge analysis of monazite and dolomite surface atoms before and after collector adsorption.

Mineral surface	Figure Number	Mulliken atomic charge (e)									
		(1)[a] Ce (in Ce–O)		(2)[a] Ce (in Ce=O)		(3)[a] –O– (from collector)		(4)[a] =O (from collector)		(5)[a] Ca (in dolomite)	
		Before	After	Before	After	Before	After	Before	After	Before	After
Monazite	5(a)	1.23	1.24	1.23	1.2	−0.58	−0.45	−0.41	−0.46	n.a.	n.a.
Dolomite	5(b)	n.a.	n.a.	n.a.	n.a.	−0.58	−0.56	−0.41	−0.5	1.5	1.58

[a] (1), (2), (3), (4) and (5) refer to marked atoms in Fig. 5.

Table 3
Mulliken charge analysis of monazite and dolomite surface atoms before and after adsorption of acid soap and oleate dimer.

Interaction system	Figure	Mulliken Charge analysis (e)											
		(1)[a] Metal atoms		(2)[a] O in C=O		(3)[a] O in C–O		(4)[a] O in C=O		(5)[a] O in C–O		(6)[a] Metal atoms	
		Before	After	Before	After	Before	After	Before	After	Before	After	Before	After
Monazite-acid soap	6(a)	1.23	1.25	−0.37	−0.4	−0.5	−0.43	−0.36	−0.4	−0.49	−0.44	1.23	1.24
Monazite-oleate dimer	7(a)	1.23	1.24	−0.23	−0.25	−0.4	−0.35	−0.22	−0.26	−0.4	−0.37	1.23	1.24
Dolomite-acid soap	6(b)	1.5	1.54	−0.37	−0.4	−0.5	−0.45	−0.36	−0.4	−0.49	−0.46	1.5	1.54
Dolomite-oleate dimer	7(b)	1.5	1.57	−0.23	0.24	−0.4	−0.38	−0.22	−0.23	−0.4	−0.36	1.5	1.57

[a] (1), (2), (3), (4), (5) and (6) refer to marked atoms in Figs. 6 and 7.

Table 4
Adsorption energies and average formed covalent bond lengths of oleate ion, acid soap and oleate dimer during interaction with dolomite (104) and monazite (100) surface.

	Monazite (100) surface			Dolomite (104) surface		
	Oleate ion	Acid soap	Oleate dimer	Oleate ion	Acid soap	Oleate dimer
Interaction energy (kJ/mol)	−422.2	−391.2	−342.1	−358.2	−332.3	−311.4
Average length of formed covalent bonds (nm)	0.223	0.221	0.246	0.258	0.254	0.296

lengths are close to the Ce–O bond length average in the monazite slab (100) structure (0.255 nm). The two active functional groups can interact with Ce through bridged binding conformations (Fig. 5(a)). The O–C=O angle of adsorbed collector on the monazite surface is 121.55° for the configuration shown in Fig. 5(a). This angle is close to the equilibrium O–C=O angle in the free oleate ion (120.14°) suggesting some degree of stability of the adsorbed species.

The interaction between C–O and C=O functional groups and Ca atoms on the dolomite surface (Fig. 5(b)) occurs via bidentate

binding conformation. The interaction energy amounts only to −352.2 kJ/mol (as seen in Table 4) and the O–Ca bond lengths are around 0.246 and 0.271 nm for C–O and C=O groups, respectively (Fig. 5(b)), which indicates less activity of C=O. This conformation between collector and Ca on the surface was obtained from several repetitions; in these simulations, Mg atoms were not approached by collector. These suggest that the C=O group in the collector and the Mg atoms on the surface are less active than the C–O group and Ca atoms. This difference in affinities is ascribed to the larger ionic radius (and lesser electronegativity) of Ca with respect to Mg. In addition, O atom in C–O group carries more negative charge as compared to C=O group, causing the former to be more reactive. The O–Ca bond lengths are around 0.246 and 0.271 nm for C–O and C=O groups, respectively (Fig. 5(b)). Both O–Ca bond lengths are larger as compared with those involved in the monazite-collector interactions. Furthermore, these distances are slightly greater than those of Ca–O and Mg–O (0.24 and 0.22 nm, respectively) on the dolomite surface structure, and confirm the chemical nature of the interaction between dolomite and oleate ion. In addition, the calculated O–C=O angle of adsorbed collector on the dolomite surface is 120.76°, which is again close to the angle of the free collector. These computed properties all concur to an interaction of oleate ion and dolomite of a chemical nature though to a with lesser strength than for monazite.

Mullikencharge analysis (Table 2) quantifies the importance of electron transfer between collector and minerals surface lattice atoms in terms of shared electrons involving HOMOs and LUMOs to give rise to covalent bonds. The C–O group oxygen atoms give up more electron charge when the oleate collector has adsorbed onto monazite than dolomite. This is coherent with the relatively more negative interaction energy between collector and monazite than dolomite (see Table 4).

3.4.2.2. Cases of oleate dimer and acid soap on monazite and dolomite surfaces. As seen in Fig. 3, oleate dimer, $(Ol)_2^{2-}$, and acid soap, $H(Ol)_2^-$, could also form in aqueous solution at pH around 7, and could likewise be adsorbed on the mineral surfaces. These three species differ from each other considering their polarity, surface activity and solubility; they are therefore expected to behave differently for the same mineral surfaces.[14] The interaction energies, the average lengths of covalent bond formed, the configuration of both oleate dimer and acid soap on the mineral have been quantified through DFT simulations.

Mulliken charge analysis of mineral surfaces before and after interaction with oleate dimer and acid soap (Table 3) suggests that the interaction should be chemisorption. Moreover, as seen in Table 4, bond lengths are relatively close to bond lengths between atoms in mineral structure (around 0.2 nm) which indicates formation of covalent bonding between oleate collector species and mineral surfaces. In Fig. 6, it can be observed that all oxygen atoms in C=O and C–O groups in acid soap interact with the metal atoms both on dolomite or monazite surfaces. This is unlike the behavior of the oleate dimer shown (Fig. 7). Three (respectively, two) out of four oxygen atoms of oleate dimer polar heads in the case of monazite (respectively, dolomite) have formed covalent bonding.

3.4.3. Adsorption of supernatant species on monazite surface

The speciation of dolomite in solution shows that various species such as $Ca(OH)_2$, $Mg(OH)_2$, $CaCO_3$, and $MgCO_3$ ion pairs or solid precipitates could precipitate out of dolomite supernatant and adsorb onto the surface of the minerals (see Section 3.3). Although the XPS results (see Figs. S3–S5) could identify only the presence of calcium and magnesium carbonates on the surface of monazite, the interaction of the hydroxide precipitate with the mineral surface was also investigated (Fig. 8). The interaction of these species with the mineral surfaces has been discussed in previous work.[9] The authors refer the readers to the previous work[9] for more details. It should also be noted that hydrated Ca^{2+}, a dissolved mineral species, could form $CaOH^+$ before adsorption on the mineral's surface.[8] In this work, Ca^{2+} adsorption on mineral's surface was the one presented since the simulation using COSMO has already considered the presence of solvation layer.

The influence of adsorption of any species on the mineral surfaces' chemical reactivity was studied through comparison of the Mullikencharge analysis. Table 5 summarizes the results for the participating atoms (both from monazite and from supernatant species) before and after supernatant species adsorption. The results show occurrence of electron transfer between the atoms during species adsorption. The results (Table 2) suggest that the metals (Ca and Mg from the adsorbed species; and Ce at the monazite surface), which are active centers for collector adsorption,[4] could be less reactive to collector species as seen from the decrease in the Mulliken charge after supernatant species adsorption.

Speciation of oleate (Fig. 3) showed that the concentration of $(Ol)^-$ was higher than the others at the studied conditions. In addition, the interaction energy of oleate ions (Table 4) with the mineral surfaces was found to be the most negative, hence the strongest. Therefore, the interactions of oleate ions with adsorbed Ca^{2+}, $Ca(OH)_2$, $CaCO_3$ and $MgCO_3$ species on the monazite surface were prioritized and are studied as shown in Fig. 9. In this figure, it can be seen that the collector's C–O and C=O groups interact with the Mg and Ca atoms from the adsorbed species through bidentate conformation. It was noted previously that the metals (Ca or Mg) from the neutral ion pairs or solid precipitates could become new collector adsorption sites on the monazite surface. Table 6 summarizes the interaction energies between sodium oleate and adsorbed $Ca(OH)_2$, $CaCO_3$, $MgCO_3$ species and Ca^{2+} ions. The interaction energies with monazite decreased in the presence of pre-adsorbed Mg and Ca bearing species from dolomite supernatant. Monazite-collector interaction with pre-adsorbed species is less favourable than in the case of bare monazite.

For further understanding of the interaction between collector and supernatant species at the monazite surface, Mullikencharge analysis was also considered. As presented in Table 5, electron transfer occurred between all atoms of the mineral surface, adsorbed supernatant species and collector polar head. This analysis shows that atoms on the minerals surface were still involved in collector interaction since their charges have been changed, even though the mineral surface was covered with new species. It was also found that sharing of electrons between collector-mineral (Table 5) occurred more than collector-adsorbed supernatant (Table 7). This finding is deduced from: (1) comparison between changes on electron charges of O in C–O and C=O groups (collector polar head) and (2) comparison between changes on electron charges of all metal atoms involved in covalent bond with either C–O or C=O groups (collector polar head).

4. Discussion

The effect of dolomite supernatant on the flotation of dolomite, monazite and bastnäsite with sodium oleate at pH 7 was investigated. Possible species from dolomite supernatant that can be formed/precipitated in the solution or at the solution/mineral interface are $MgCO_3$, $CaCO_3$, $Mg(OH)_2$ and $Ca(OH)_2$ based from the equilibrium equations and speciation diagram of dolomite supernatant (see Eqs. S1–S17 and Fig. S2). However, among these, only the carbonate precipitates were observed at surface of the minerals through XPS analyses (see Figs. S3–S5). The deviation could be attributed to the conditioning time used in this experiment, which

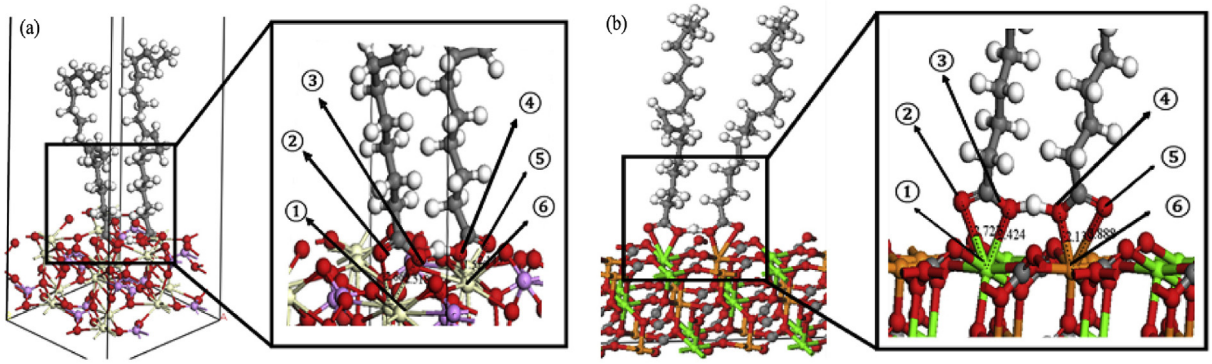

Fig. 6. Interaction of acid soap onto monazite surface (100) (a) and dolomite surface (104) (b) (Ce ≡beige, O ≡ red, P ≡ purple, C ≡ gray, Mg ≡ orange, Ca ≡ green, H ≡ white).

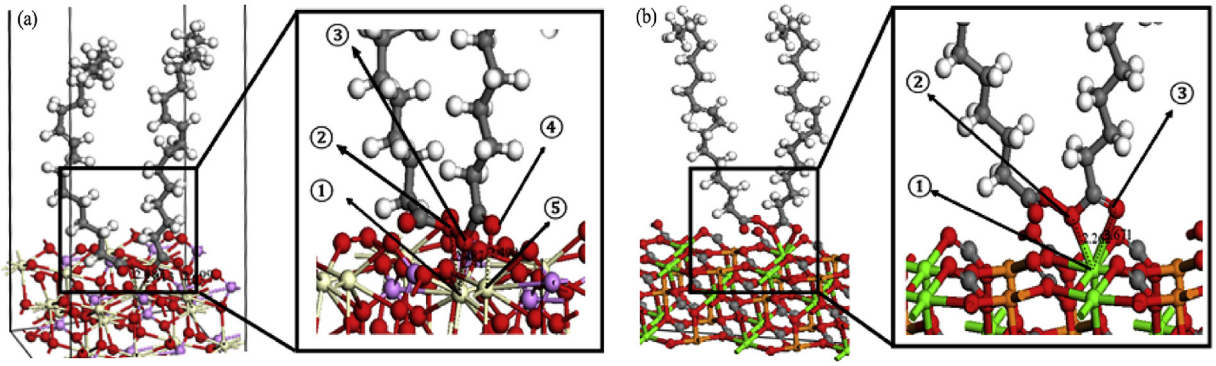

Fig. 7. Interaction of oleate dimer onto monazite surface (100) (a) and dolomite surface (104) (b) (Ce ≡beige, O ≡ red, P ≡ purple, C ≡ gray, Mg ≡ orange, Ca ≡ green, H ≡ white).

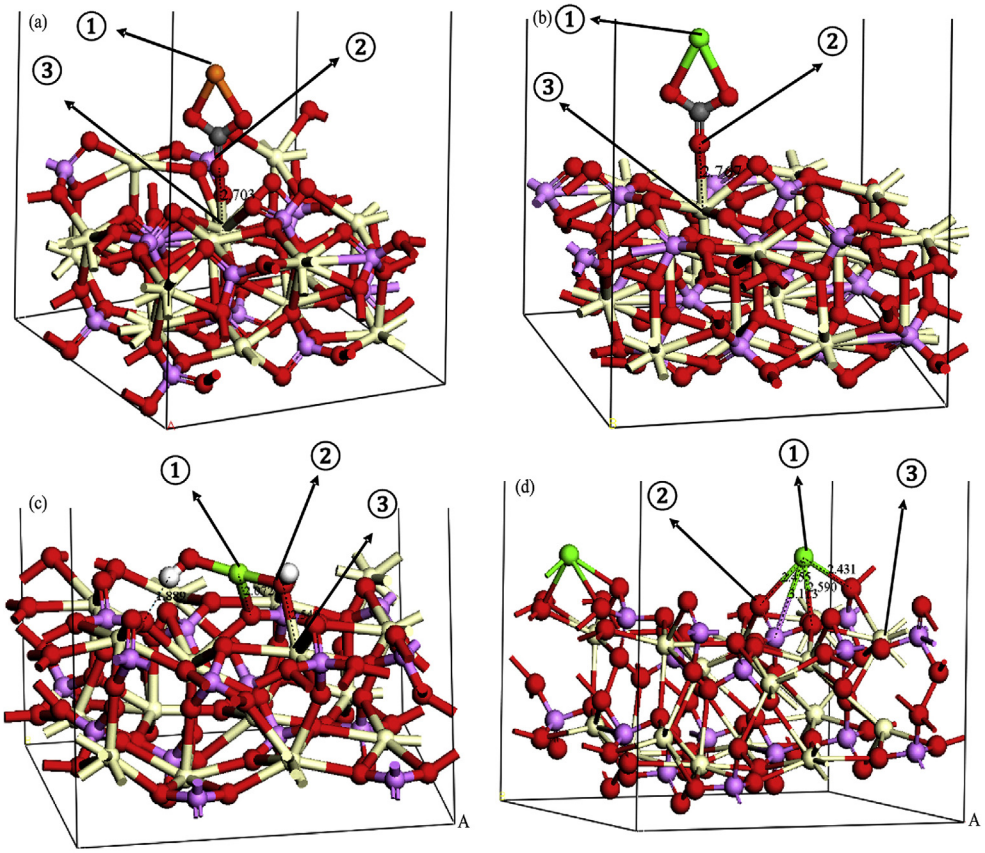

Fig. 8. Interaction of $MgCO_3$ (a), $CaCO_3$ (b), $Ca(OH)_2$ (c) and Ca^{2+} (d) ions on the monazite surface (100) (Ce ≡beige, O ≡ red, P ≡ purple, C ≡ gray, Mg ≡ orange, Ca ≡ green, H ≡ white).

Table 5
Mulliken population analysis of monazite surface atoms before and after supernatant species adsorption.

Adsorbed species	Figure Number	Mulliken atomic charge (e)					
		(1)[a] Metal from supernatant species (Ca/Mg)		(2)[a] O in O–Ce		(3)[a] Ce from monazite	
		Before	After	Before	After	Before	After
$MgCO_3$	8(a)	1.86	1.36	−0.71	−0.41	1.23	1.15
$CaCO_3$	8(b)	1.72	1.65	−0.67	−0.41	1.23	1.14
$Ca(OH)_2$	8(c)	2	1.45	−1.2	−0.92	1.23	1.16
Ca^{2+}	8(d)	2	1.43	−0.67	−0.79	1.23	1.20

[a] (1), (2) and (3) refer to marked atoms in Fig. 8.

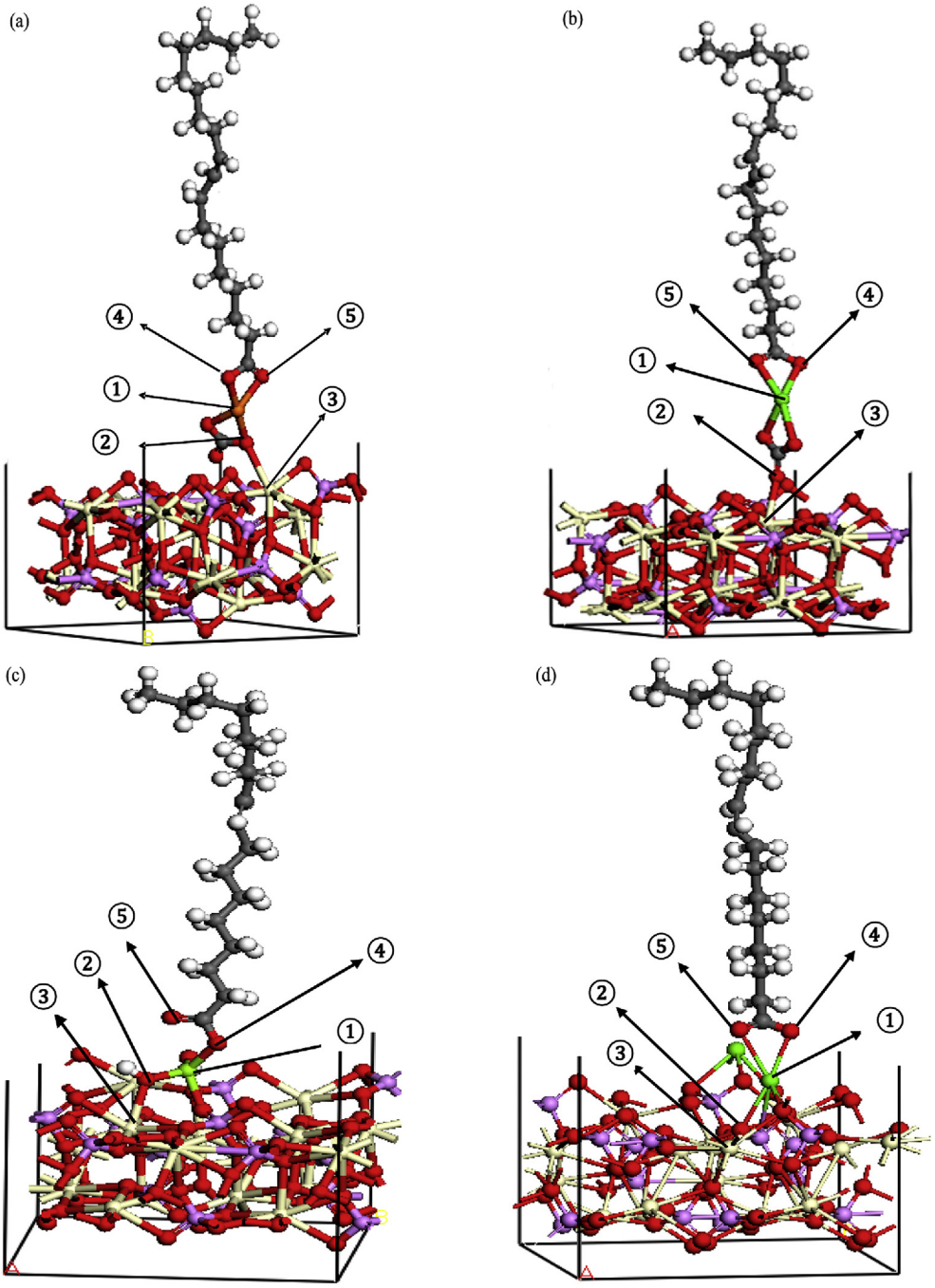

Fig. 9. Interaction of collector with species $MgCO_3$ (a), $CaCO_3$ (b), $CaOH_2$ (c), and Ca^{2+} (d) at the monazite surface (100) (Ce ≡ beige, O ≡ red, P ≡ purple, C ≡ gray, Mg ≡ orange, Ca ≡ green, H ≡ white).

Table 6
Adsorption energy of oleic acid onto dolomite (104) and monazite (100) surface active centers with and without precipitated supernatant species.

Component	Interaction energy (kJ/mol)					
	On bare dolomite (104) surface	On bare monazite (100) surface	Adsorbed supernatant species on the monazite (100) surface			
			$MgCO_3$	$CaCO_3$	$Ca(OH)_2$	Ca^{2+}
Collector	−358.2	−422.2	−326.5	−335.1	−320.2	−356.4

Table 7
Mullikencharge analysis of monazite with adsorbed supernatant species before and after collector adsorption.

Adsorbed species	Figure Number	Mulliken atomic charge (e)									
		(1)[a] Ca or Mg (from adsorbed species)		(2)[a] O (in Ce–O)		(3)[a] Ce from monazite		(4)[a] –O– (from collector)		(5)[a] =O (from collector)	
		Before	After	Before	After	Before	After	Before	After	Before	After
$MgCO_3$	9(a)	1.36	1.4	−0.56	−0.67	1.23	1.15	−0.58	−0.56	−0.41	−0.56
$CaCO_3$	9(b)	1.65	1.63	−0.41	−0.48	1.23	1.14	−0.58	−0.55	−0.41	−0.56
$Ca(OH)_2$	9(c)	1.45	1.37	−0.89	−0.91	1.23	1.16	−0.58	−0.57	−0.41	−0.43
Ca^{2+}	9(d)	1.43	1.56	−0.79	−0.78	1.23	1.06	−0.58	−0.56	−0.41	−0.57

[a] (1), (2), (3), (4) and (5) refer to marked atoms in Fig. 9.

could be shorter than the time needed for the hydroxides to precipitate. Other species found at the surface of the minerals through XPS analyses are $>CaOH^0$ (dolomite) and $>CO_3H^0$ (bastnäsite). These are expected as carbonate minerals when exposed to water tend to form these surface sites.[29]

4.1. The interaction of the mineral surface with oleate ion, acid soap and oleate dimer

Before interpreting the effect of the supernatant on the mineral surface, the interaction of the different oleate species in the solution will be discussed first. Since oleate can dissociate in the solution into oleate ion, Ol^-, acid soap, $H(Ol)_2^-$, and oleate dimer, $(Ol)_2^{2-}$,[14] these three species were investigated through DFT simulation. The calculations showed that all the C–O and C=O groups of the oleate ion and acid soap are involved in the interaction with the mineral surface through covalent bonding (see Section 3.4.2). However, for the oleate dimer, only 3 out of 4 O atoms are engaged in the collector-monazite interaction (Fig. 7(a)); while, only 2 O atoms are involved in the collector-dolomite interaction (Fig. 7(b)). This kind of configuration may indicate that acid soap interacts more strongly with the mineral surfaces compared with oleate dimer. This can also be confirmed through comparison between interaction energies and the average lengths of formed covalent bonds during mineral-collector species interactions (Table 4). Since shorter average bond lengths reflect stronger interaction, it can be validated that the interaction of acid soap is more favorable than oleate dimer with both monazite and dolomite. Other studies also suggested that acid soap is more stable and surface active than the dimer because of the absence of charge repulsion.[12] An assessment between the oleate ion (monomer) and the dimer was not made by these authors due to the contrasting influence of the size and the charge. In this study, considering the HOMOs and LUMOs, no direct comparison between oleate ion and the dimer can also be made. However, it confirms that acid soap should interact more with the minerals than with the dimer, as well as than oleate ion. Though it suggests that acid soap should be more reactive than oleate ion, contrary to what was proposed in the literature,[12] Mulliken charge of the O atom in C–O (which is involved in the collector-mineral interaction), suggests that oleate ion (Table 2) has stronger interaction with the minerals than acid soap (Table 3). Also, on the basis of calculated interaction energies provided in Table 4, it can be observed that the strength of the interaction on the mineral surfaces is greater (indicated by more negative interaction energy) for oleate ions $(Ol)^-$ than acid soap $H(Ol)_2^-$; and acid soap is greater than oleate dimer $(Ol)_2^{2-}$.

4.2. The effect of dolomite supernatant on the zeta potential of the minerals

When the minerals are conditioned with only NaOl, the zeta potential of the minerals became greatly negative (Fig. 1), suggesting that the dissociated forms of the collector have strong interaction with the bare mineral surface. The adsorption of negatively charged oleate species at the surface of negatively charged dolomite surface, confirms the chemisorbing characteristic of the collector at this pH condition.[11] In addition, DFT simulations (Table 4) showed that the bond lengths of O–Ca interacting with the C–O and C=O groups of the collector are slightly exceeding the bond lengths of Ca–O and Mg–O on dolomite surface, indicating that the interaction of dolomite and the collector is chemical by nature. The results of Mullikencharge analysis also confirmed the chemical nature of collector-mineral interaction by presenting that electron sharing (charge exchanges) occurs between atoms of collector and mineral (Tables 2 and 3). Electrostatic forces also appeared to have an important role in the adsorption of the collector due to the differences between the zeta potential before (presence of NaCl) and after conditioning with NaOl; it can be observed that the interaction with sodium oleate is stronger for bastnäsite, followed by monazite and then dolomite. This correlates well with the zeta potential of bare mineral surface: bastnäsite is 9.8 eV > monazite is −0.6 eV > dolomite is −10.4 eV, and in agreement with calculated interaction energies demonstrated in Table 4.

Zeta potential measurements (Fig. S1) showed that conditioning with dolomite supernatant in the presence of NaOl collector significantly affects the minerals (particularly the RE minerals) at basic pH. This is expected as the cations (from dolomite supernatant) start to form precipitates at these pH conditions.[25] Since the effect of dolomite supernatant was already investigated at pH 9,[9] the authors decided to investigate further the consequences of the dissolved mineral species at pH 7. Additionally, previous studies have shown that maximum recovery of RE minerals in the presence of oleate occurred close to this pH.[15,16] Additional zeta potential

measurements were conducted with the minerals in the presence of only 1×10^{-3} mol/L NaCl, and only supernatant (Fig. 1). When the negatively-charged dolomite was exposed to the supernatant, zeta potential became less negative. This could be due to the adsorption of positively-charged species such as Ca^{2+} or $CaOH^{+}$ as suggested by speciation diagram (see Fig. S2) and as confirmed by XPS analyses (see Figs. S3–S5). However, when monazite and bastnäsite were pulped with the supernatant, the zeta potential reduced significantly (see Fig. 1). At pH 7, the zeta potential of the main precipitated species $MgCO_3$, is slightly negative[30]; moreover, HCO_3^- species from the supernatant could also make the surface of the bastnäsite negative and monazite more negative.[25] These negatively charged species ($MgCO_3$ and HCO_3^-) could interact more with the positively charged surface of bastnäsite than with the slightly negative monazite and negatively charged dolomite, as can be seen from the zeta potential values (Fig. 1). This was also supported by the XPS results, which show that the increase in the amount of $>HCO_3^0$ can be observed at the surface of bastnäsite after conditioning with the supernatant (Fig. S3).

4.3. The effect of dolomite supernatant on minerals' flotation

The minerals' zeta potential (Fig. 1) agreed with the flotation results (Fig. 2), which showed that the RE minerals have higher floatability than dolomite in deionised water. It appears that both electrostatic forces and chemical interactions between collector and minerals were more promoted in the case of RE minerals resulting in higher flotation recoveries (Fig. 2). Although oleate is a strong collector, and is known to be nonselective, the DFT simulations still show that this collector has stronger interaction with monazite than dolomite (Table 4). By comparing the changes in the atomic charge by Mulliken analyses (see Table 2), it can be seen that the O in C–O (which has more coordinating ability than O in C=O) participated more in the monazite-collector interaction than in the dolomite-collector interaction. Compared to previous finding with benzohydroxamate collector,[9] the presence of dolomite supernatant also had detrimental effect to monazite and bastnäsite flotation with sodium oleate, (considered to be) a strong collector. In the presence of dissolved mineral species, it can be observed that bastnäsite is more affected than monazite, while monazite is more affected than dolomite (Fig. 2). As mentioned previously, electrostatic interaction might play an important role in the adsorption of negatively charged precipitate and ionic species onto the surface of the minerals. Since bastnäsite is positively charged and monazite is less negative than dolomite (see Fig. 1), these RE minerals have more affinity to these species, making their surface adsorb more of these species than that of dolomite. In addition, the floatability of bastnäsite and monazite is expected to be more affected, since the precipitated species-collector interaction is less favourable than bare mineral-collector interaction, as suggested by the calculated interaction energies (Table 6). Dolomite might have some species precipitated at its surface as well, which would explain why dolomite recovery was also slightly affected. Another reason for the decrease in flotation recovery could be the formation of Ca- and Mg-oleate precipitate (Fig. 3) in the solution. The precipitation of these species could have led to a decrease in the available oleate for mineral interaction, thus a decrease in recovery.

4.4. Sodium oleate compared with benzohydroxamate (aromatic RE collector)

Based on these results, oleate can be considered a stronger collector than typical RE mineral collector, benzohydroxamate (an aromatic hydroxamate). As seen from the calculated interaction energies (Table 4) and by the results from the previous work (see Table 8),[9] mineral-oleate interaction energies are more negative (hence, stronger) than mineral-benzohydroxamate interaction energies. This is highly influenced by the chain length of sodium oleate, since the length of the hydrophobic radical influences the level of hydrophobicity that the collector provides to the mineral.[2] Increasing the chain length of the collector makes it a stronger collector but less selective.[2] The difference between the interaction energies of dolomite and monazite are also observed to be smaller (Table 4) with sodium oleate than benzohydroxamate (see Table 8), indicating that benzohydroxamate is a more selective collector than sodium oleate. The degree of selectivity can be explained by the polarity of the O in N–O (benzohydroxamate) and C–O (oleate) groups, which are involved in the collector-mineral interactions. Since N is more electronegative than C, O in N–O will have lesser negative charge (−0.48e)[9] than O in C–O (−0.58e) (see Section 3.4.1). The lesser negative charge of O in N–O makes it more selective for interaction with metals than O in C–O. Interestingly, the calculated interaction energies show that there was only a slight difference between monazite-benzohydroxamate and monazite - oleate interaction, while a significant difference was observed between dolomite-benzohydroxamate and dolomite-oleate interactions. This observation can be attributed to the surface structure of the minerals and the collector. The Ce atoms at the monazite surface are more reactive than the Ca and Mg atoms at the dolomite surface, however the combined site densities of Ca and Mg are greater than that of Ce. Moreover, because of the aromatic chain of the benzohydroxamate, it will have more steric hindrance effect than oleate which has a linear chain. It means that oleate can approach the mineral surfaces more easily than benzohydroxamate. Since more reactive oleate can interact easier with more exposed active centers of dolomite, then the difference in interaction energy between monazite-benzohydroxamate and monazite - oleate could be significantly less compared to the difference between dolomite-benzohydroxamate and dolomite-oleate.

5. Conclusions

Sodium oleate is a popular collector for RE minerals, and though it is also known to have strong affinity to carbonate minerals such as dolomite; the presence of dolomite supernatant still shows to have decreased the floatability of RE minerals. It is found that at pH 7, the dissolved and precipitated dolomite species such as hydrated Ca^{2+}, $CaCO_3$ and $MgCO_3$ might adsorb at the surface of the minerals. The adsorbed species-collector interaction is slightly lesser than dolomite-collector interaction, and dolomite-collector is lesser

Table 8
Adsorption energy of benzohydroxamate collector on dolomite (104) surface and monazite (100) surface active centers with and without precipitated supernatant species.[9]

Component	Interaction energy (kJ/mol)					
	On dolomite (104) surface	On bare monazite (100) surface	Adsorbed supernatant species on the monazite (100) surface			
			$MgCO_3$	$CaCO_3$	$Ca(OH)_2$	Ca^{2+}
Collector	−184.4	−385.5 −330.3	−190.2	−187.7	−177.4	−200.4

than monazite-collector interaction, reflecting the decrease in the mineral's recovery in the presence of dolomite supernatant. Moreover, thermodynamic calculations indicated that precipitation of oleate as Ca-oleate and Mg-oleate can occur at pH 7, which could also be a reason for a decrease in recovery.

When compared to aromatic hydroxamate collectors, the strength and non-selectivity of sodium oleate collector could be mostly attributed to its structure and the gangue's structure. The oleate's strength as a collector is mostly attributed to its long hydrocarbon chain, which imparts hydrophobic characteristic to the mineral. The low selectivity is attributed to oleate's lower steric hindrance effect and has higher reactive O atom involved in the interaction. The dolomite's structure, which presents more exposed active sites to the collector than those of RE minerals also influences the ease at which the collector approaches the mineral's surface-active sites.

DFT simulations of the oleate ion, acid soap and dimer have also been presented in this work. Although the importance of acid soap in the flotation has been emphasized in the literature, in this work, the simulations indicate that oleate ion is the most important species due to its strong interaction with the mineral surface. It can be proposed that oleate ion is adsorbed onto the mineral surface through a strong covalent interaction. Due to the lack of charge repulsion from undissociated oleate (HOl), it can adsorb to the initially adsorbed oleate ion through hydrogen bonding, forming an acid soap at the mineral surface. Further investigations by DFT simulations must be conducted to understand the mechanism of formation/adsorption of the acid soap on the mineral surface.

Acknowledgements

The authors would like to acknowledge Natural Sciences and Engineering Research Council of Canada (NSERC) and Niobec, a Magris Resources Company for funding this research through the Collaborative Research and Development Program (CRDPJ 453164-13). The authors would also like to acknowledge McGill Engineering Doctoral Award for partial funding of E.R.L. Espiritu and G.R. da Silva. We are also indebted to Compute Canada for the HPC platform without which the DFT simulations would not have been possible.

Appendix A. Supplementary data

Supplementary data related to this article can be found at https://doi.org/10.1016/j.jre.2018.04.016.

References

1. Bulatovic SM. Handbook of flotation reagents: chemistry, theory and practice. In: *Flotation of sulfide ores*. vol. 1. Elsevier; 2007.
2. Wills BA, Finch JA. Froth flotation. In: Finch JA, Wills BA, eds. *Wills' mineral processing technology*. 8th ed. Boston: Butterworth-Heinemann; 2016:265.
3. Jordens A, Cheng YP, Waters KE. A review of the beneficiation of rare earth element bearing minerals. *Miner Eng*. 2013;41:97.
4. Yang ZR, Bian X, Wu WY. Flotation performance and adsorption mechanism of styrene phosphonic acid as a collector to synthetic $(Ce,La)_2O_3$. *J Rare Earths*. 2017;35(6):621.
5. Li M, Gao K, Zhang DL, Duan HJ, Ma LL, Huang L. The influence of temperature on rare earth flotation with naphthyl hydroxamic acid. *J Rare Earths*. 2018;36(1):99.
6. Fuerstenau, Jameson GJ, Yoon R-H. *Froth flotation: a century of innovation*. Littleton, CO: SME; 2007.
7. Zhang X, Du H, Wang XM, Miller JD. Surface chemistry considerations in the flotation of rare-earth and other semisoluble salt minerals. *Miner Metall Process*. 2013;30(1):24.
8. Zhang WC, Honaker RQ, Groppo JG. Flotation of monazite in the presence of calcite part I: calcium ion effects on the adsorption of hydroxamic acid. *Miner Eng*. 2017;100:40.
9. Espiritu ERL, da Silva GR, Azizi D, Larachi F, Waters KE. The effect of dissolved mineral species on bastnäsite, monazite and dolomite flotation using benzohydroxamate collector. *Colloids Surf, A*. 2018;539:319.
10. Predali J. Flotation of carbonates with salts of fatty acids: role of pH and the alkyl chain. *Trans Inst Min Metall*. 1969;78:C140.
11. Fuerstenau MC, Miller JD. The role of the hydrocarbon chain in anionic flotation of calcite. *Trans AIME*. 1967;238(2):153.
12. Somasundaran P, Ananthapadmanabhan K. Solution chemistry of surfactants and the role of it in adsorption and froth flotation in mineral-water systems. In: Mittal KL, ed. *Solution chemistry of surfactants*. vol. 2. New York, NY: Plenum; 1979:17.
13. Pugh R, Stenius P. Solution chemistry studies and flotation behaviour of apatite, calcite and fluorite minerals with sodium oleate collector. *Int J Miner Process*. 1985;15(3):193.
14. Kulkarni RD, Somasundaran P. Flotation chemistry of hematite/oleate system. *Colloids Surf, A*. 1980;1(3):387.
15. Gerdel M, Smith R. The role of lignin sulfonate in flotation of bastnasite from barite. In: Bautista RG, Wong MM, eds. *Rare earths, extraction, preparation and applications*. TMS; 1988.
16. Dixit S, Biswas A. pH-Dependence of the flotation and adsorption properties of some beach sand minerals. *Trans Soc Mining Eng AIME*. 1969;244(2):173.
17. Pradip Rai B, Rao TK, Krishnamurthy S, Vetrivel R, Mielczarski J, Cases JM. Molecular modeling of interactions of diphosphonic acid based surfactants with calcium minerals. *Langmuir*. 2002;18(3):932.
18. Pradip Rai B. Molecular modeling and rational design of flotation reagents. *Int J Miner Process*. 2003;72(1–4):95.
19. Rai B, Pradip. Design of highly selective industrial performance chemicals: a molecular modelling approach. *Mol Simulat*. 2008;34(10–15):1209.
20. Rai B. *Molecular modeling for the design of novel performance chemicals and materials*. New York, NY: CRC Press; 2012.
21. Rath SS, Sinha N, Sahoo H, Das B, Mishra BK. Molecular modeling studies of oleate adsorption on iron oxides. *Appl Surf Sci*. 2014;295:115.
22. Ataman E, Andersson MP, Ceccato M, Bovet N, Stipp SLS. Functional group adsorption on calcite: I. Oxygen containing and nonpolar organic molecules. *J Phys Chem C*. 2016;120(30):16586.
23. Ataman E, Andersson MP, Ceccato M, Bovet N, Stipp SLS. Functional group adsorption on calcite: II. Nitrogen and sulfur containing organic molecules. *J Phys Chem C*. 2016;120(30):16597.
24. Prédali J-J, Cases J-M. Zeta potential of magnesian carbonates in inorganic electrolytes. *J Colloid Interface Sci*. 1973;45(3):449.
25. Chen G, Tao D. Effect of solution chemistry on flotability of magnesite and dolomite. *Int J Miner Process*. 2004;74(1–4):343.
26. Gans P. *Hyperquad simulation and speciation (HySS)*. Leeds, England: Protonic Software; 2009.
27. Bonnitcha PD, Kim BJ, Hocking RK, Clegg JK, Turner P, Neville SM, et al. Cobalt complexes with tripodal ligands: implications for the design of drug chaperones. *Dalton Trans*. 2012;41(37):11293.
28. Albright TA, Burdett JK, Myung-Hwan Whangbo. *Orbital interactions in chemistry*. Hoboken, NJ: John Wiley & Sons; 2013.
29. Van Cappellen P, Charlet L, Stumm W, Wersin P. A surface complexation model of the carbonate mineral-aqueous solution interface. *Geochem Cosmochim Acta*. 1993;57(15):3505.
30. Škvarla J, Kmet S. Non-equilibrium electrokinetic properties of magnesite and dolomite determined by the laser-Doppler electrophoretic light scattering (ELS) technique. A solids concentration effect. *Colloids Surf, A*. 1996;111(1):153.